PERGAMON

Acta mater. 48 (2000) 3545–3551

Acta MATERIALIA

www.elsevier.com/locate/actamat

PLASTIC VERSUS ELASTIC DEFORMATION EFFECTS ON MAGNETIC BARKHAUSEN NOISE IN STEEL

C.-G. STEFANITA, D. L. ATHERTON and L. CLAPHAM†

Department of Physics, Queen's University, Kingston, Ontario K7L 3N6, Canada

(Received 2 February 2000; received in revised form 10 March 2000; accepted 19 April 2000)

Abstract—A study was performed to differentiate the effects of elastic and plastic deformation on magnetic Barkhausen noise (MBN) signals. Linear and angular MBN measurements were made on a number of mild steel plate samples subjected to varying degrees of uniaxial elastic and plastic deformation up to ~40% strain. Elastic strain effects on the MBN_{energy} were determined to be far more significant than plastic strain effects. MBN_{energy} increases in the early plastic deformation region were attributed to a slight increase in elastic strain due to work hardening. Magnetic anisotropy studies indicated that elastic strain significantly alters the magnetic anisotropy (α) in the sample, but changes the isotropic signal (β) very little. Plastic deformation has a smaller, but apparently opposite effect, in that it appears to change β but has little influence on α. As plastic deformation levels become large, however, behaviour becomes more complex and is less well understood. © *2000 Acta Metallurgica Inc. Published by Elsevier Science Ltd. All rights reserved.*

Keywords: Magnetic methods; Steel; Mechanical properties—elastic and plastic

1. INTRODUCTION

Magnetic Barkhausen noise (MBN) occurs when a changing magnetic field is applied to a ferromagnetic material, and is due to irreversible domain wall motion across local pinning sites. The high sensitivity of MBN to elastic strain [1–7] has made it an effective tool for investigating deformation in ferromagnetic materials. The few published papers dealing with plastic strain effects on MBN [8–12] reveal inconsistent results due to the use of different materials and MBN signal interpretation. However, the findings of these independent studies display one common feature: MBN response to plastic strain is quite different to that of elastic strain. The present paper examines the MBN behaviour of mild steel deformed up to and beyond the yield point, and after unloading. A more detailed discussion of MBN response to stress below the macroscopic yield point is discussed in another paper [13].

2. THEORETICAL BACKGROUND

2.1. MBN measurements

The present study employed two different types of surface MBN measurements. The first type, termed "linear MBN" are measurements taken along a linear trajectory on a sample surface. At each location, the measured MBN voltage spectrum is analyzed by integrating the time dependence of the voltage squared signal to arrive at a parameter termed the "MBN_{energy}" [14]. The second type of measurement, called "angular MBN" is used to characterize the magnetic anisotropy of a polycrystalline sample. Measurements are performed at a single location by rotating the excitation field magnet in 10° increments from one measurement to the next. MBN_{energy} is once again used to characterize the signal, but is displayed in polar form as a function of angle. The polar MBN_{energy} result can be described by:

$$MBN_{energy} = \alpha \cos^2(\theta - \phi) + \beta \qquad (1)$$

where θ is the angle of the applied magnetic field with respect to the reference (rolling or axial) direction; α is associated with the angular dependent variation of the MBN signal; β with the angular independent signal (isotropic background); and ϕ is the direction of the magnetic easy axis with respect to the reference direction. The maximum of the angular dependent MBN measurements corresponds to the bulk magnetic easy axis direction (ϕ) of the sample.

† To whom all correspondence should be addressed.

E-mail address: lynann@physics.queensu.ca (L. Clapham).

PII: S1359-6454(00)00134-8

2.2. Elastic stress effects

We have conducted a number of studies of elastic strain effects on magnetic easy axis behaviour in pipeline steel and steel plates [5–7, 14]. These studies have shown that an applied elastic tensile stress increases MBN_{energy} and creates a strong magnetic easy axis in the stress direction. Conversely, other studies [15] have shown that an applied compressive elastic stress decreases the MBN_{energy} in the compression direction, thus creating a magnetic easy axis perpendicular to the applied stress. The stress dependence of the MBN-monitored magnetic easy axis has been attributed to the changes in the domain wall configuration in response to an applied stress, as described in earlier work [7].

2.3. Plastic deformation effects

Plastic deformation creates a significant increase in dislocation density and movement of dislocations leading to dislocation tangles. These dislocation tangles are believed to act as pinning sites to domain wall movement [8, 9]. Figure 1 illustrates how domain wall energy might be affected by plastic deformation [16, 17]. Figure 1(a) shows the domain wall energy variation with wall position before plastic deformation. The pressure exerted by the field H applied at an angle ψ with respect to domain magnetization M_s tends to move the wall across pinning site 1, unless this pressure is counterbalanced by the wall energy gradient [16]

$$\frac{\partial E_w}{\partial x} = 2M_s H \cos\psi \qquad (2)$$

Further increase of the field results in an irreversible domain wall "jump" to pinning site 2, a position with larger wall energy gradient. At still higher fields, the domain wall moves to pinning site 3. Successive domain wall displacements across pinning sites occur until the wall energy gradient is large enough to prevent further motion of the wall.

With increased internal stress, the critical field required to move a domain wall across a pinning site, and implicitly the wall energy gradient, increase [16, 17]. Dislocation tangles are energetically significant enough to produce effective pinning sites for domain walls [8, 9]. Dislocation density increases during plastic deformation lead to changes in domain wall energy gradient at pinning sites. Inhomogeneous distortion of a crystal lattice results in large shear displacements occurring on widely separated slip planes, while regions between these slip planes remain almost undeformed [18]. As a result, the domain wall energy gradient increases at some pinning sites, while remaining essentially the same at others. This is illustrated in Fig. 1(b), where there is an increase in energy gradient at sites 1 and 3 but not 2. An applied field, sufficient to overcome site 1, enables the wall to jump directly to site 3, moving past 2 without being pinned by it. This is expected to result in a correspondingly larger MBN response compared to that resulting from the situation in Fig. 1(a).

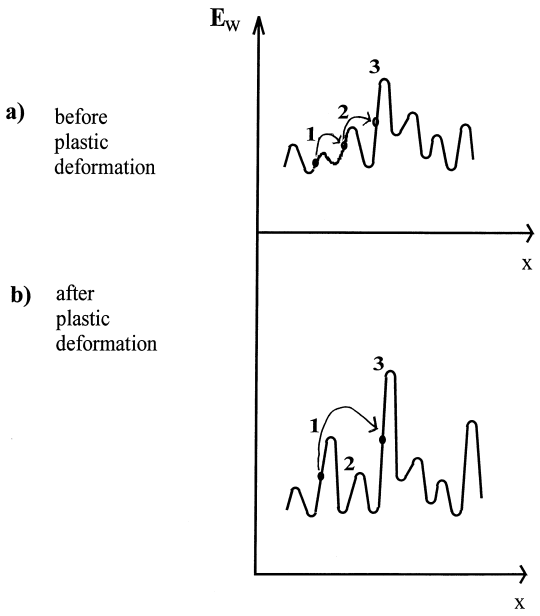

Fig. 1. Variation of domain wall energy as a function of the position of the wall. Energy distribution at pinning sites (a) before and (b) after plastic deformation.

3. EXPERIMENTAL TECHNIQUE

The specimens were obtained from a 3 mm thick hot rolled mild steel plate with a yield point of ~190 MPa (determined by a 0.2% offset method), and a Young's modulus of 167 GPa. Pole figures constructed using X-ray diffraction showed a random distribution of crystallographic planes. Tensile specimens of central dimensions 260 mm (L) × 57 mm (W) × 3 mm (T) were cut from the mild steel plate such that the stress direction coincided with the rolling direction of the plate. Two different apparatus were used to apply a uniaxial stress to the samples. The first, built specifically for combining stress and MBN testing [13] allowed MBN measurements to be made when stress was being applied; unfortunately the loading limit on this unit corresponded to only about 14% strain in the samples. The second apparatus, a Riehle Uniaxial Testing machine, enabled much higher stress levels to be achieved in the samples (up to ~40% strain), but unfortunately it was not possible to make MBN measurements during stress application. Samples stressed in this apparatus were therefore stressed, unloaded and removed for MBN testing. Since the elastic strain is removed with unloading, the MBN results for these tests predominately reflect the effect

Table 1. Successive loading and unloading cycles for specimens under uniaxial tensile stress. The maximum strain reached during loading is indicated, as well as the plastic strain present after unloading

Specimen	Cycle 1		Cycle 2		Cycle 3	
	Maximum strain reached during loading (%)	Plastic strain after unloading (%)	Maximum strain reached during loading (%)	Plastic strain after unloading (%)	Maximum strain reached during loading (%)	Plastic strain after unloading (%)
1	0.13	0.03	0.87	0.63	–	–
2	1.55	1.43	–	–	–	–
3	2.88	2.74	–	–	–	–
4	0.12	0.02	3.55	3.41	39.98[a]	39.69

[a] Necking.

of plastic deformation. Four samples were stressed repeatedly to higher deformation levels using this apparatus. Table 1 details the loading and unloading cycles for the four specimens. The final cycle on sample 4 involved deformation up to necking (~40%).

A schematic illustration of the apparatus used for MBN measurements is shown in Fig. 2. The MBN signal is excited using a sweep field magnet made of a ferrite U-core wound with ~800 turns of fine wire. The excitation is provided by a 12 Hz sine wave signal produced by a waveform generator and a bipolar power supply. The core assembly also includes a coil or read head detector situated between the magnet pole pieces. The detected signal is preamplified, filtered using a 3–200 kHz bandpass filter, and then fed into an RC Electronics Computerscope. Due to skin depth considerations, MBN is primarily a surface technique with the detected MBN signal originating from depths less than ~0.2 mm below the surface. An earlier study [19] examined the effects on MBN of surface grinding with SiC papers and found no change in the MBN signals for grit sizes smaller than 600 grade SiC. For this reason all sample surfaces were carefully ground to a 600 SiC grit finish prior to MBN measurement.

4. RESULTS

4.1. MBN results for samples subjected to applied uniaxial loading in tension

Figure 3 shows the effect of progressively increasing tensile strain on angular MBN results. The solid lines through the data represent the fit of equation (1) to the experimental result. Figure 3(a) illustrates that prior to deformation the sample displays no magnetic anisotropy; however the application of an elastic stress to 0.2% (the approximate yield point) creates a significant magnetic easy axis in the stress direction. This behaviour is consistent with other studies of steel plate materials [20]. Continued tensile deformation above the yield point enhances the easy axis [Fig. 3(b)], but at a much lower rate (per unit stress) than in the elastic region. This is further illustrated by examining the variation of fitting parameters α and β [from the

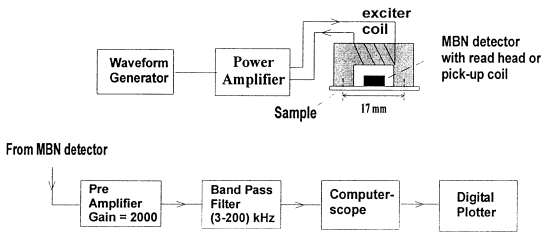

Fig. 2. Block diagram of experimental apparatus for producing and detecting magnetic Barkhausen noise.

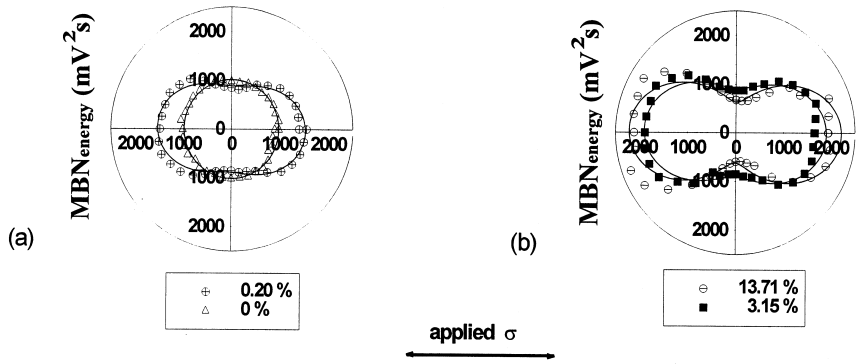

Fig. 3. Selected polar plots of angular MBN_{energy} illustrating (a) undeformed and fully elastic (0.2%) strain states, and (b) strain into the plastic regime. Solid lines are curves of best fit described by equation (1).

equation (1) fit to the data] with strain. Figure 4 shows these variations, plotted on two different strain scales in order to illustrate more clearly the behaviour in each of the elastic and plastic regions. These curves indicate that the β parameter, which is associated with the isotropic background of the MBN signal, remains essentially constant throughout the deformation process. Conversely, the α parameter, representing the magnetic anisotropy, increases progressively with increased deformation. Figure 4 further illustrates that α has a much greater strain dependence in the elastic, compared to the plastic, deformation region.

The trends in Figs 3 and 4 are reinforced by "average MBN_{energy}" results shown in Fig. 5(a) and (b). The results in Fig. 5 are obtained by averaging individual MBN_{energy} values obtained at points along a linear trajectory on the sample subjected to various levels of deformation. As in earlier diagrams, a much stronger MBN dependence on strain is seen in the elastic, compared to the plastic, deformation region. This is the case for detector orientations both parallel and transverse to the stress direction.

4.2. MBN results for unloaded samples

Figure 6 shows α and β parameters obtained from angular MBN measurements on unloaded samples, with α and β shown as a function of the plastic strain in the sample after unloading. It should be noted that the large difference in scale between these α and β results compared to those seen in Fig. 4 is primarily due to a somewhat different MBN setup in each case. Figure 6 shows that α, which reflects the magnetic anisotropy, changes little until the plastic strain becomes very large. Conversely, the β parameter has a significant plastic strain dependence, initially increasing and then decreasing at very large deformations.

Figure 7 shows the average MBN_{energy} obtained along a linear trajectory [similar to that plotted in Figs 5(a) and (b)], for the unloaded samples, again as a function of plastic strain after unloading. In this case both detector orientations show similar results, with the average MBN_{energy} initially increasing and then decreasing at very high plastic stress levels.

Finally, the pulse height distribution of the MBN

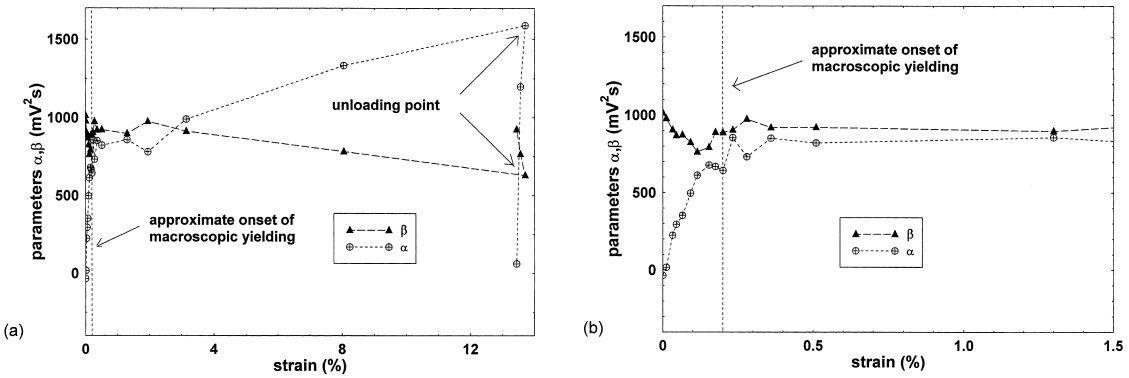

Fig. 4. Variation with strain of fitting parameters α and β of equation (1); (a) overall behaviour throughout the deformation cycle, and (b) expanded strain region to 2% strain. Connecting dashed lines are only for guidance.

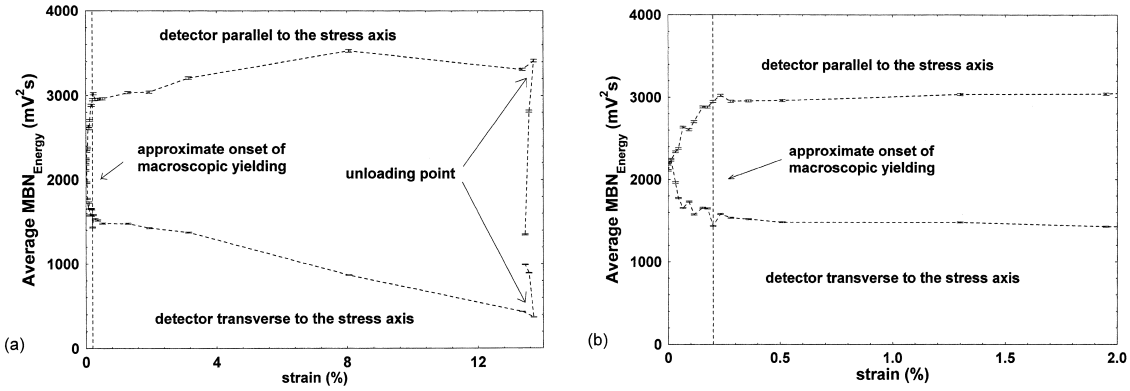

Fig. 5. Summary of average MBN_{energy} data along an axial scan; (a) overall behaviour throughout the deformation cycle, and (b) expanded strain region to 2% strain. Connecting dashed lines are only for guidance.

signal was examined for a few of the unloaded samples, for detector orientations parallel to [Fig. 8(a)] and at 40° to [Fig. 8(b)] the stress axis. A significant increase in the "tail" of the distribution curve (larger voltage pulses) is observed at an angle of 40° to the applied stress axis [Fig. 8(b)]. This is close to the direction of maximum shear stress. The directions parallel [Fig. 8(a)], and transverse (not shown) display a less pronounced increase in the tail with applied stress.

5. DISCUSSION

5.1. Elastic deformation effects on MBN

Elastic deformation has been shown to have a significant influence on MBN behaviour. This results from changes in the domain configuration in response to changes in the interatomic spacing, described as follows [after 7]. Steel generally has a positive magnetostriction coefficient, i.e. it is energetically favourable for domain magnetization vectors to lie along the ⟨100⟩ direction that is closest to an applied tensile stress direction. Therefore in response to an applied stress, the domains within individual grains must reorient to minimize their energy. Two possible mechanisms have been proposed to explain the response of the domain pattern to an applied stress in single crystals, based on the energy changes associated with the relative volume of 180° and 90° domains. The first involves a reorientation of 180° domains into the ⟨100⟩ direction that is closest to the stress direction. The second mechanism involves an increase in the 180° domain wall population, for domains that lie in or close to the stress direction. A combination of these two mechanisms implies that a tensile stress will create more domain walls in the stress direction, and a compressive stress fewer walls in the stress direction. Since MBN is associated with the pinning of these domain walls as they move during magnetization, the MBN signal is predicted to increase in the direction of tensile stress, and decrease in the direction of compressive stress.

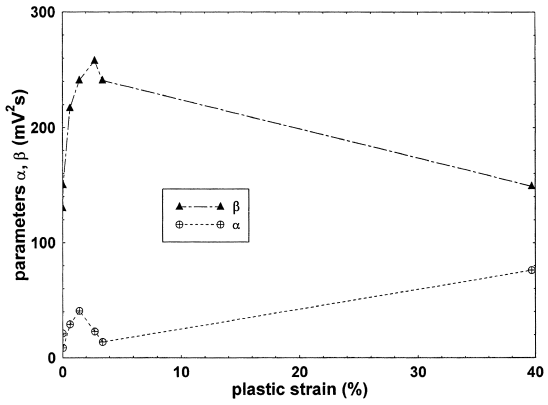

Fig. 6. Behaviour of fitting parameters α and β of equation (1) throughout the entire plastic strain range. Connecting dashed lines are only for guidance.

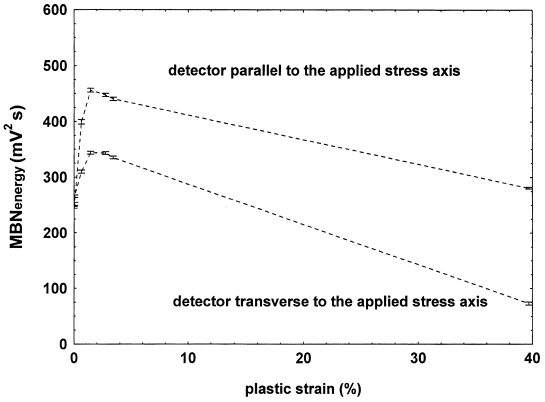

Fig. 7. Summary of average MBN_{energy} data (measured after unloading) for the entire plastic strain range investigated. Measurements were made for detector orientations parallel and transverse to the applied stress direction. Connecting dashed lines are only for guidance.

5.2. Plastic deformation effects on MBN

The main conclusion to be drawn from the present study, as illustrated in Figs 3–5, is that the MBN signal is far less dependent on plastic deformation than it is on elastic deformation, although there is still a small strain dependence in the plastic range. The reason for the difference in effect between the two types of strain lies in the fact that they occur by two different mechanisms. As discussed above, elastic strain involves an increase or decrease in the atomic spacing and therefore affects the magnetic behaviour directly through magnetoelastic energy considerations. Once the plastic regime is reached, however, the macroscopic elastic strain remains approximately constant, with plastic deformation occurring through slip processes. These processes lead to a number of changes that potentially can alter magnetic behaviour:

1. an increase in the number of microscopic pinning sites in the form of dislocation tangles and cell boundaries, which act as obstacles to domain wall movement,
2. development of a crystallographic texture, which may alter the magnetic easy axis, direction, and finally
3. additional, minor local elastic stress increases in the plastic region associated with the work hardening processes [21].

It is difficult to estimate quantitatively the degree to which each of these contributes to a change in the MBN signal. However, it is interesting that the relationship between MBN_{energy} and strain shown in Fig. 5(a) (for the detector parallel to stress) is very similar in form to the engineering stress vs engineering strain curve obtained during a standard tensile test of the specimen material (not shown here). The similar form of the two plots led us to combine them to produce a graph of MBN_{energy} vs engineering stress (Fig. 9). Interestingly, Fig. 9 shows that a line of best fit represents equally well the data from the elastic and plastic regions of the curve. This provides strong evidence that the minor MBN sensitivity to stress in the early part of the plastic regime (up to ~13% strain) is due to additional small elastic stress increases. We believe this to be a result of work hardening, explained as follows: In the elastic region, stress is accommodated by an increase in atomic spacing of the lattice. Potentially this spacing increase can continue until fracture, however at some critical stress value "slip systems" within the material are activated and the material begins plastic flow. As plastic deformation progresses, however, dislocation generation and interaction leads to work hardening [21]. Work hardening slightly increases the critical value for slip, thus allowing slightly more elastic stress to be accommodated in the crystal lattice through increases in lattice spacing.

The results of Figs 3–5 provide evidence that the slight increase in MBN_{energy} within the early part of the plastic regime can be accounted for by considering the small increases in elastic stress that accompany plastic deformation. However, as deformation proceeds beyond this point, it is likely that the pin-

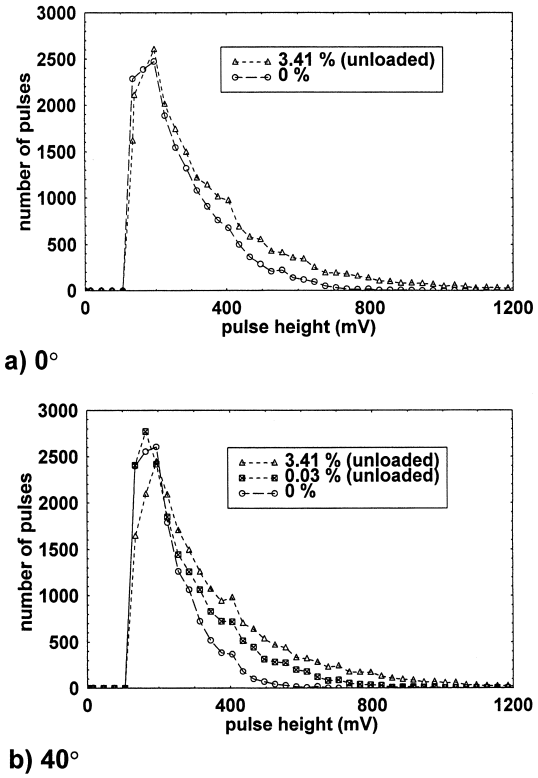

Fig. 8. Pulse height distributions for selected plastic strain levels for a detector orientation (a) parallel, and (b) at 40° to the applied stress direction.

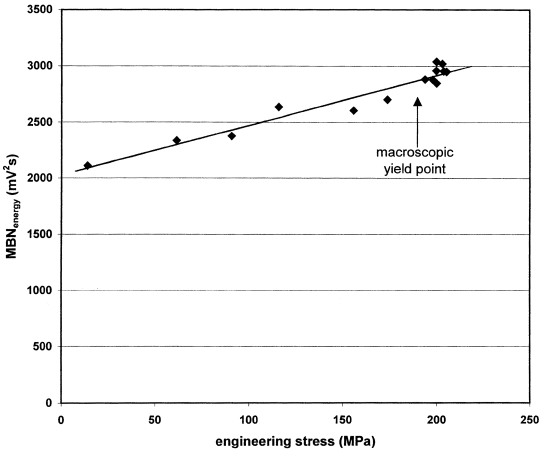

Fig. 9. Plot of MBN_{energy} as a function of engineering stress, obtained by combining the results of Fig. 5(a) (detector parallel to stress) with the information from the engineering stress/engineering strain curse for the sample.

ning effects of dislocation tangles become increasingly important. In contrast to elastic effects, which increase α (magnetic anisotropy) but leave β (the isotropic signal level) essentially unchanged [Fig. 4(b)], plastic deformation appears to alter β more than α. This is illustrated in Fig. 6. It also explains why results from both MBN detector orientations show similar responses to increasing plastic strain in Fig. 7. A remaining question, however, is why the MBN_{energy} diminishes significantly at high levels of plastic strain, as seen in Fig. 7. This may be a result of competition between plastic deformation and crystallographic texture effects, and is part of a continuing investigation.

Finally, the pulse height distributions in Fig. 8 warrant further comment. The pinning site arguments presented in the section on plastic deformation effects, suggest that larger MBN pulses are produced as plastic deformation alters the relative energies of adjacent pinning sites. This may explain the behaviour seen in Fig. 8. Both (a) and (b) illustrate that plastic deformation increases the number of large MBN events, with this behaviour being most evident near the direction of maximum shear stress [Fig. 8(b)].

6. CONCLUSIONS

An examination of the effects of both elastic and plastic deformation effects on MBN signals has shown that elastic effects are far more significant. Elastic strain significantly alters the magnetic anisotropy (α) in the sample, but changes the isotropic signal (β) very little. Plastic deformation has a smaller, but apparently opposite effect, in that it appears to change β but has little influence on α. Furthermore, the evidence suggests that the MBN_{energy} increases in the early plastic deformation region are likely a result of a slight increase in elastic strain due to work hardening. As plastic deformation levels become large, however, behaviour becomes more complex and is less well understood.

REFERENCES

1. Altpeter, I., Theiner, W. A. and Reimringer, B., in *Residual Stresses, Proc. Eur. Conf. Res. Str*, ed. E. Macherauch and V. Hauk. DEM-Verlag, Karlsruhe, 1983, p. 263.
2. Clapham, L., Krause, T. W., Olsen, H., Ma, B. and Atherton, D. L., *NDT&E Int*., 1995, **28**(2), 73.
3. Dhar, A. and Atherton, D. L., *NDT&E*, 1993, **10**, 287.
4. Gauthier, J., Krause, T. W. and Atherton, D. L., *NDT&E Int*., 1998, **31**(1), 23.
5. Jagadish, C., Clapham, L. and Atherton, D. L., *IEEE Trans. Magn*., 1989, **25**(5), 3452.
6. Jagadish, C., Clapham, L. and Atherton, D. L., *NDT Int*., 1989, **22**(5), 297.
7. Krause, T. W., Clapham, L., Pattantyus, A. and Atherton, D. L., *J. Appl. Phys*., 1996, **79**(8), 4242.
8. Birkett, A. J., Corner, W. D., Tanner, B. K. and Thompson, S. M., *J. Phys. D: Appl. Phys*., 1989, **22**, 1240.
9. Hwang, D. G. and Kim, H. C., *J. Phys. D: Appl. Phys*., 1988, **21**, 1807.
10. Krause, T. W. and Atherton, D. L., Magnetic Barkhausen noise measurements on non-oriented Si–Fe steel. Unpublished work, 1993.
11. Lieneweg, U., *IEEE Trans. Magn*., 1974, **MAG-10**, 118.
12. Yi, J.-K., Nondestructive evaluation of degraded structural materials by micromagnetic technique. Ph.D. thesis, Korea Adv. Inst. Sci & Tech., Dept. of Nucl. Eng., Taejon, Korea, 1993.
13. Stefanita, C.-G., Clapham, L. and Atherton, D. L., Subtle changes in magnetic Barkhausen noise before the macroscopic elastic limit. *J. Mat. Sci*., 1999, accepted for publication.
14. Krause, T. W., Clapham, L. and Atherton, D. L., *J. Appl. Phys*., 1994, **75**(12), 7983.
15. Krause, T. W., Makar, J. M. and Atherton, D. L., *J. Mag.and Mag. Materials*, 1994, **137**, 25.
16. Chikazumi, S., *Physics of Magnetism*. Wiley, New York, 1964.
17. Bozorth, R. M., *Ferromagnetism*. IEEE Press, New York, 1951.
18. Kittel, C., *Introduction to Solid State Physics*. Wiley, New York, 1986.
19. Clapham, L., Jagadish, C. and Atherton, D. L., *Acta metall. mater*., 1991, **39**, 1555.
20. Clapham, L., Heald, C., Krause, T. W., Atherton, D. L. and Clark, P., *J. Appl. Phys*., 1999, accepted for publication.
21. Dieter, G. E., *Mechanical Metallurgy*, 3rd ed. McGraw-Hill, New York, 1986.